Fermilab Library
0 1160 0038643 7

259

MIDWESTERN UNIVERSITIES RESEARCH ASSOCIATION

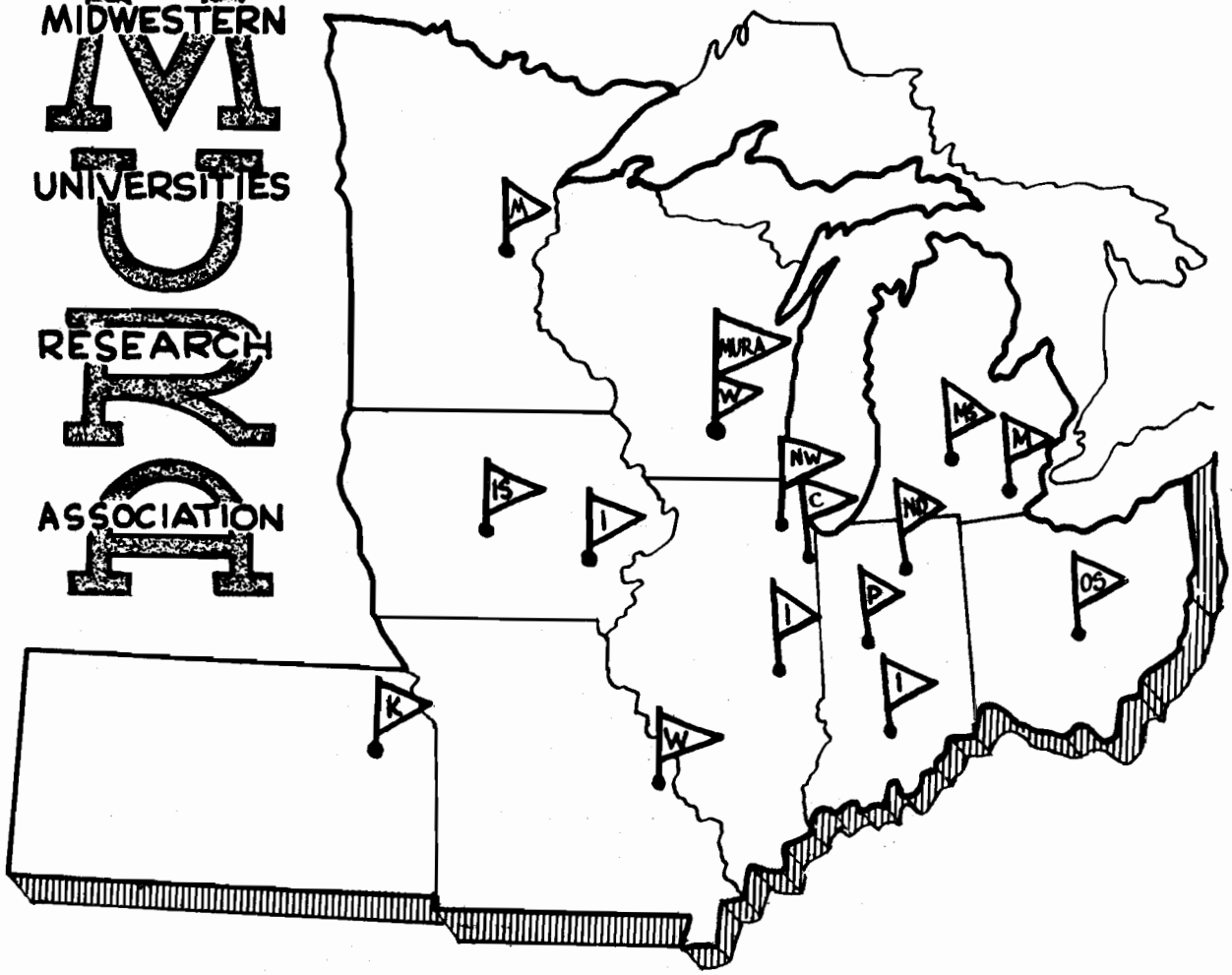

FIELDS IN GAP-EXCITED RECTANGULAR DUCTS

J. Van Bladel

REPORT **NUMBER** 259

MURA-259
Internal

MIDWESTERN UNIVERSITIES RESEARCH ASSOCIATION*

2203 University Avenue, Madison, Wisconsin

FIELDS IN GAP-EXCITED RECTANGULAR DUCTS

J. Van Bladel

May 4, 1957

ABSTRACT: The electromagnetic field in a rectangular waveguide, cut in two by a plane perpendicular to its longitudinal axis, is investigated. A voltage applied across the two halves of the guide generates the field structure, which is being analyzed for several values of frequency (allowed to vary between zero and cut-off) and of aspect ratio of the cross-section. The problem is of interest for the design of particle accelerators.

* Supported by Contract AEC #AT (11-1)-384

I. INTRODUCTION

The accelerating fields in a particle accelerator are often excited by means of a gap-impressed voltage (Figure 1). Detailed knowledge of the resulting field structure is of interest for the exact computation of particle trajectories. It is the purpose of this paper to give a description of the field for the following conditions:

1. The curvature of the vacuum-chamber is negligible, and the chamber can be considered as a straight portion of wave-guide with perfectly conducting walls.

2. The vacuum-chamber has a rectangular cross-section, the shape of which could eventually be very "flat". Flat accelerator tubes with aspect ratios of twenty or more are being considered for the Fixed Field Alternating Gradient machines now under study at the Midwestern Universities Research Association.

3. The frequency of the gap voltage is lower than the cut-off frequency $c/2a$ of the guide. This condition is normally satisfied in accelerators.

4. The gap is so narrow that the detailed distribution of the tangential electric field on its surface is immaterial. It will be assumed, in particular, that external sources impress a tangential field of the form $\underset{\sim}{E}_{\hat{t}} = V_0 \cos \omega t \cdot \delta(z)\, \underset{\sim}{u}_{\hat{z}}$ across the gap opening (see Figure 2).

II. MATHEMATICAL SOLUTION OF THE PROBLEM

The electric field $\underset{\sim}{E}$ within a volume V containing no charges and currents, is uniquely determined by the tangential component of the field at the boundary surface S. The mathematical formula allowing actual computation of $\underset{\sim}{E}$ is:

$$\underset{\sim}{E}(\underset{\sim}{r}_{\hat{0}}) = \iint_S \left[\underset{\sim}{n} \times \underset{\sim}{E}(\underset{\sim}{r}_{\hat{s}})\right] \cdot \operatorname{curl} \Gamma_{\hat{t}}(\underset{\sim}{r}_{\hat{s}} | \underset{\sim}{r}_{\hat{0}})\, dS \qquad (2.1)$$

where $\underset{\sim}{r}_{\hat{0}}$ is the radius vector of the field point, $\underset{\sim}{r}_{\hat{s}}$ is the radius vector of a point on S, $\underset{\sim}{n}$ is the unit vector along the outward normal to S, and Γ_t is the transverse (i.e. solenoidal) part of Green's dyadic[1] relative to region V. Green's dyadic $\Gamma(\underset{\sim}{r} | \underset{\sim}{r}_{\hat{0}})$ is defined by the equations:

$$\nabla^2 \Gamma(\underset{\sim}{r} | \underset{\sim}{r}_{\hat{0}}) + k^2 \Gamma(\underset{\sim}{r} | \underset{\sim}{r}_{\hat{0}}) = \mathcal{J}\, \delta(\underset{\sim}{r} - \underset{\sim}{r}_{\hat{0}}) \qquad (2.2)$$

$$\underset{\sim}{n} \cdot \Gamma(\underset{\sim}{r}_{\hat{s}} | \underset{\sim}{r}_{\hat{0}}) = 0$$

where $\mathcal{J}$ is the identity dyadic, and $k^2 = \omega^2/c^2 = (2\pi/\lambda)^2$. Green's dyadic and its solenoidal part, are fortunately available in close analytical form for the infinitely long rectangular wave-guide.[2] The curl of $\Gamma_{\hat{t}}$, the quantity of interest in the computation of the electric field, turns out to be:

$$\operatorname{curl} \Gamma_{\hat{t}}(\underset{\sim}{r} | \underset{\sim}{r}_{\hat{0}}) = -\frac{k^2}{2ab} \sum_{m=0}^{\infty} \sum_{n=0}^{\infty} \frac{\varepsilon_{\hat{m}}\, \varepsilon_{\hat{n}}}{\gamma^2_{\hat{m},n} (\gamma^2_{\hat{m},n} - k^2)^{1/2}} \Big\{ \operatorname{curl}\left[e^{-(\gamma^2_{\hat{m},n} - k^2)^{1/2} |z - z_{\hat{0}}|} \underset{\sim}{B}_{\hat{m},n}(x,y) \right] \underset{\sim}{B}_{\hat{m},n}(x_{\hat{0}}, y_{\hat{0}})$$
$$+ \operatorname{curl}\left[e^{-(\gamma^2_{\hat{m},n} - k^2)^{1/2} |z - z_{\hat{0}}|} \underset{\sim}{C}_{\hat{m},n}(x,y) \right] \underset{\sim}{C}_{\hat{m},n}(x_{\hat{0}}, y_{\hat{0}}) \Big\} \qquad (2.3)$$

---

1) For general background material on Green's dyadic, see:
P.M. Morse and H. Feshbach, Methods of Theoretical Physics (McGraw Hill Co., New York, 1953) Ch. 13.

F. E. Borgnis und C. H. Papas, Randwertprobleme der Mikrowellenphysik (Springer Verlag, Berlin, 1955) pp 251 and ff.

2) P.M. Morse and H. Feshbach, loc. cit., pp. 1819 to 1825.

This formula is valid only when the guide is below cut-off, i.e. $k^2 < (\pi/a)^2$

Some clarification of the symbols is necessary:

1. ε_k is Neumann's factor, equal to one for K=0, to two for $K>0$
2. $\gamma^2_{m,n}$ is equal to $\left(\frac{m\pi}{a}\right)^2 + \left(\frac{n\pi}{b}\right)^2$, m and n being integers.
3. $\underset{\sim}{B}_{m,n}(x,y) = \frac{n\pi}{kb}\cos\frac{m\pi x}{a}\sin\frac{n\pi y}{b}\,\underset{\sim}{u}_x - \frac{m\pi}{ka}\sin\frac{m\pi x}{a}\cos\frac{n\pi y}{b}\,\underset{\sim}{u}_y$
4. $\underset{\sim}{C}_{m,n}(x,y) = \frac{(\gamma^2_{m,n} - k^2)^{1/2}}{k^2}\cdot\left[\frac{m\pi}{a}\cos\frac{m\pi x}{a}\sin\frac{n\pi y}{b}\,\underset{\sim}{u}_x + \frac{n\pi}{b}\sin\frac{m\pi x}{a}\cos\frac{n\pi y}{b}\,\underset{\sim}{u}_y\right]$
$$+ \frac{\gamma^2_{m,n}}{k^2}\sin\frac{m\pi x}{a}\sin\frac{n\pi y}{b}\,\underset{\sim}{u}_z$$

When the expression for curl Γ_t is introduced in equation (2.1), together with the assumed value for the tangential component of $\underset{\sim}{E}$, the following expressions are being found for the components of the electric field:

$$E_z = \frac{8V}{\pi^2}\sum_{m=1,3,\ldots}^{\infty}\sum_{n=1,3,\ldots}^{\infty}\sin\frac{m\pi x}{a}\sin\frac{n\pi y}{b}\,\frac{\gamma^2_{m,n}}{mn(\gamma^2_{m,n}-k^2)^{1/2}}\cdot e^{-(\gamma^2_{m,n}-k^2)^{1/2}|z|}\cdot\cos\omega t$$

$$E_x = \mp\frac{8V}{\pi a}\sum_{m=1,3,\ldots}^{\infty}\sum_{n=1,3,\ldots}^{\infty}\cos\frac{m\pi x}{a}\sin\frac{n\pi y}{b}\cdot\frac{1}{n}\cdot e^{-(\gamma^2_{m,n}-k^2)^{1/2}|z|}\cdot\cos\omega t$$

$$E_y = \mp\frac{8V}{\pi b}\sum_{m=1,3,\ldots}^{\infty}\sum_{n=1,3,\ldots}^{\infty}\sin\frac{m\pi x}{a}\cos\frac{n\pi y}{b}\cdot\frac{1}{m}\cdot e^{-(\gamma^2_{m,n}-k^2)^{1/2}|z|}\cdot\cos\omega t \qquad (3.4)$$

The upper and lower signs correspond to positive and negative values of z respectively. It will be noticed that modes with odd quantum numbers m and n are the only ones excited. In particular, the lowest mode, often referred to as the $TE_{1,0}$ mode, is not excited.

The components of the magnetic field are easily determined by means of Maxwell's equations. One finds:

$$H_x = -\frac{8\omega\varepsilon_0 V}{\pi b}\sum_{m=1,3,..}^{\infty}\sum_{n=1,3,..}^{\infty}\sin\frac{m\pi x}{a}\cos\frac{n\pi y}{b}\cdot\frac{1}{m(\gamma^2_{m,n}-k^2)^{\frac{1}{2}}}\,e^{-(\gamma^2_{m,n}-k^2)^{\frac{1}{2}}|z|}\cdot\sin\omega t$$

$$H_y = -\frac{8\omega\varepsilon_0 V}{\pi a}\sum_{m=1,3,..}^{\infty}\sum_{n=1,3,..}^{\infty}\cos\frac{m\pi x}{a}\sin\frac{n\pi y}{b}\cdot\frac{1}{n(\gamma^2_{m,n}-k^2)^{\frac{1}{2}}}\,e^{-(\gamma^2_{m,n}-k^2)^{\frac{1}{2}}|z|}\cdot\sin\omega t$$

$$H_z = 0$$

The last equation shows that the assumed tangential field distribution does not excite the transverse electric modes.

It will be noticed that the following parity properties apply to the various field components in quadrants I to IV (Figure 2).

a) E_z is of equal parity in all four quadrants

b) E_x and H_y are of equal parity in I and II, of opposite parity in I and III, I and IV.

c) E_y and H_x are of equal parity in I and IV, of opposite parity in I and II, I and III.

The parity with respect to z is clearly indicated in formulas (2.4) and (2.5).

III. NUMERICAL RESULTS

The fields have been computed for a range of values of the following parameters:

1. The aspect ratio $\tau = a/b$ of the cross section, which, in certain graphs, was allowed to go up to $\tau = 25$, a value which could conceivably be used in the MURA machine.

2. The frequency, expressed in terms of the cut-off frequency $f_{\hat{c}} = c/2a$

3. The position of the field point, as determined by a system of axes OX, OY, OZ (see Figure 2).

It would take thousands of man-hours to compute the hundreds of double infinite sums necessary to cover the desired range of parameters. This enormous amount of human work was greatly reduced by the use of an IBM 704 computer. Only part of the computed information will be presented here, because of obvious space-limitations. The following comments will be useful in the interpretation of Figures 3 to 14.

1. <u>Longitudinal component of the electric field</u>.

The variation of $E_{\hat{z}}$ along certain lines, and throughout certain cross-sections, is depicted in Figures 3 to 6. It will be noticed that lengths are expressed in terms of a, the guide width, and electric fields in terms of V/a. The following qualitative features are apparant from the graphs:

(a) The "penetration depth" of the field on both sides of the gap is of the order of $b/2$.

(b) The field exhibits more and more of a δ function behavior as one comes closer and closer to the gap. This zone of "gap influence" increases in relative importance, of course, as the vacuum-chamber becomes flatter and flatter.

(c) The frequency dependence decreases as the guide becomes flatter, until frequency independence is practically achieved for aspect ratios of the order of five.

Similar qualitative features will be found for the other field components. The information contained in Figures 3 to 6 should allow intelligent interpolation between values of frequency and aspect ratio.

2. Transverse components of the electric field.

Both components, E_x and E_y, vanish along the main axis, and in the plane of the gap. The transverse electric field is directed along OX or OY for points situated in the OXZ and the OYZ planes respectively. Variation of E_x and E_y along various lines is depicted in Figures 7 to 9.

3. Magnetic Field.

The magnetic field is expressed in terms of $Y_0 \, V/a$, a quantity having the proper dimentions A/m. The symbol Y_0 stands for the characteristic admittance of vacuum, equal to $(\varepsilon_0/\mu_0)^{\frac{1}{2}}$. Both components, H_x and H_y, vanish along the main axis and increase monotonically as one proceeds toward the walls. Variation of H_x and H_y in the plane of the gap, and along various lines, is depicted in figures 10 to 12.

4. Additional Comments.

Various information of interest to the physicist can be derived from the knowledge of the field components. Two examples are given in Figures 13 and 14. In the former, the electric field is displayed at a few points of the OXZ plane, in a manner which suggests the curvature of the lines of force and the rate of variation of the magnitude in various directions. In the latter, the quantity $\int_{-\infty}^{+\infty} E_z \, dZ$ is being displayed along two lines. This quantity represents the voltage to which a particle would be submitted if it went through

the field region in a time short as compared to the period $2\pi/\omega$. It appears from the curves that if one volt, say, is applied across the gap, up to 2.54 volts may be "seen" by the particle if the cross-section is sufficiently square, and the frequency sufficiently close to cut-off. The additional voltage can be accounted for in terms of magnetic fluxes linking the particle trajectory.

ACKNOWLEDGMENT

The important task of programming the computation of the double infinite sums has been ably performed by Mr. J. McNall.

List of Figure Captions.

Fig. 1 Vacuum-chamber with gap-impressed voltage.

Fig. 2 Coordinate axes used in the solution of the problem.

Fig. 3 Variation of E_z along the main axis $(X = Y = 0)$ for different aspect ratios of the cross-section. The four curves for $\tau = 1$ and $\tau = 2$ correspond, starting from below, to frequencies $0, f_c/2, 3f_c/4$ and f_c. The two curves for $\tau = 5$ correspond to frequencies 0 and f_c, while for $\tau = 10$ and 25 the curves are practically overlapping for all frequencies between zero and cut-off.

Fig. 4 Variation of E_z along the main axis ($X = Y = 0$), and along an axis parallel to the latter, but situated halfway toward the narrow face of the guide ($X = a/4$, $Y = 0$). Peaked curves correspond to $\tau = 5$, flat curves to $\tau = 1$. Fields are time-independent.

Fig. 5 Variation of E_z throughout the plane of the gap. The magnitude of the field is expressed in terms of V/a. Full lines correspond to zero frequency, dashed lines to cut-off.

Fig. 6 Variation of E_z along the OX axis for a square cross-section, and for three values of Z. Full lines correspond to zero.frequency, dashed lines to cut-off.

Fig. 7 Variation of Ex along parallels to OZ drawn in the center of the narrow face ($X = a/2$, $Y = 0$, bracketed set of curves), and halfway between the latter and the main axis ($X = a/4$, $Y = 0$). The lower curve for $\tau = 1$ and $\tau = 2$ refers to zero frequency, the upper one to cut-off. Values of Ex for $\tau = 5$ are negligible in the lower set of curves.

Fig. 8 Variation of E_y along parallels to OZ drawn in the center of the broad face ($X=0, Y=b/2$, bracketed set of curves), and halfway between the latter and the main axis ($X=0, Y=b/4$). Curves for $\tau = 1$ are identical with those of Figure 7. In each set, the lower curve for $\tau = 2$ refers to zero-frequency, the upper one to cut-off.

Fig. 9 Variation of E_x along the OX axis for a square cross-section, and for two values of Z . Full lines correspond to zero frequency, dashed lines to cut-off.

Fig. 10 Magnetic field at various points in the plane of the gap. Dashed vectors correspond to cut-off frequency, full vectors to half that frequency. For $\tau = 5$, there is proportionality between field and frequency, and vectors relative to the cut-off frequency only are displayed.

Fig. 11 Variation of H_y along a parallel to OZ drawn in the center of the narrow face ($X = a/2$, $Y = 0$, upper part of the figure) and halfway between the latter and the main axis ($X=0, Y=b/4$, lower part of the figure). In each figure, and for each value of τ , the upper curve corresponds to cut-off frequency, the lower one to half that frequency.

Fig. 12 Variation of H_x along a parallel to OZ drawn in the center of the broad face ($X=0$, $Y=b/2$, bracketed set of curves) and halfway between the latter and the main axis ($X=0, Y=b/4$). For each value of τ , the upper curve corresponds to cut-off frequency, the lower one to half that frequency.

Fig. 13 Electric field at various points in the OXZ plane.

Fig. 14 Voltage applied to a fast particle travelling (a) along the main axis ($X=Y=0$) (b) along a parallel to the latter halfway toward the narrow wall ($X = a/4$, $Y=0$).

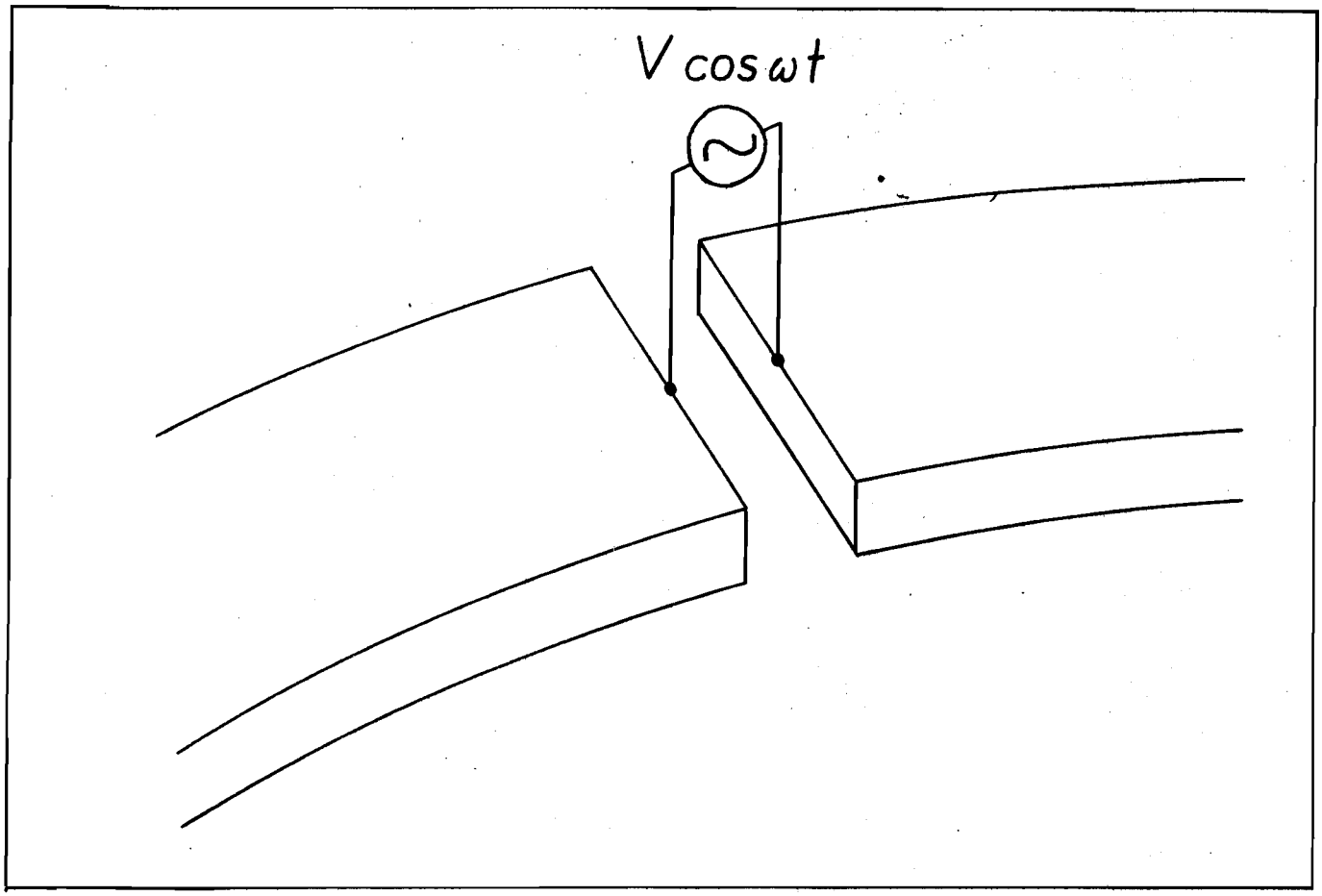

Fig. 1

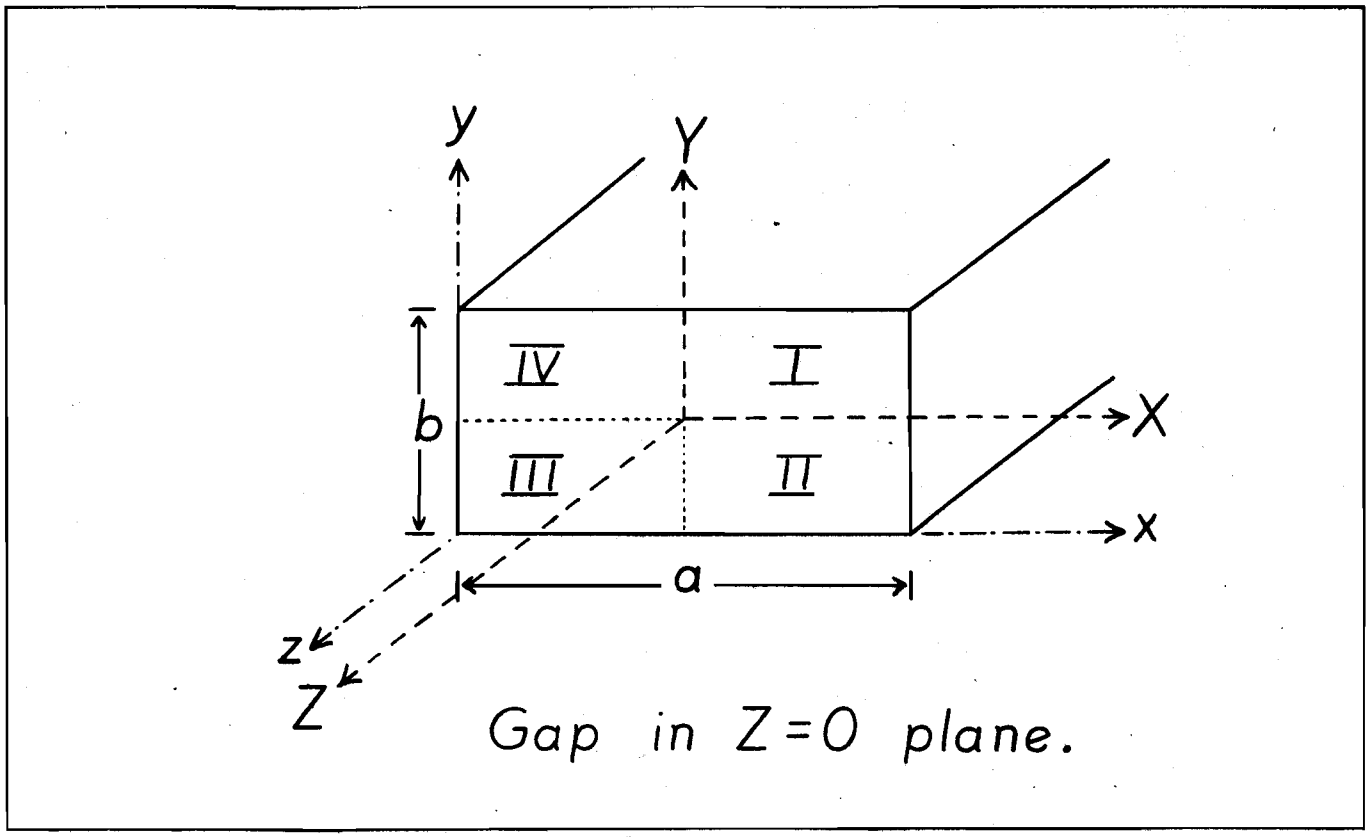

Fig. 2

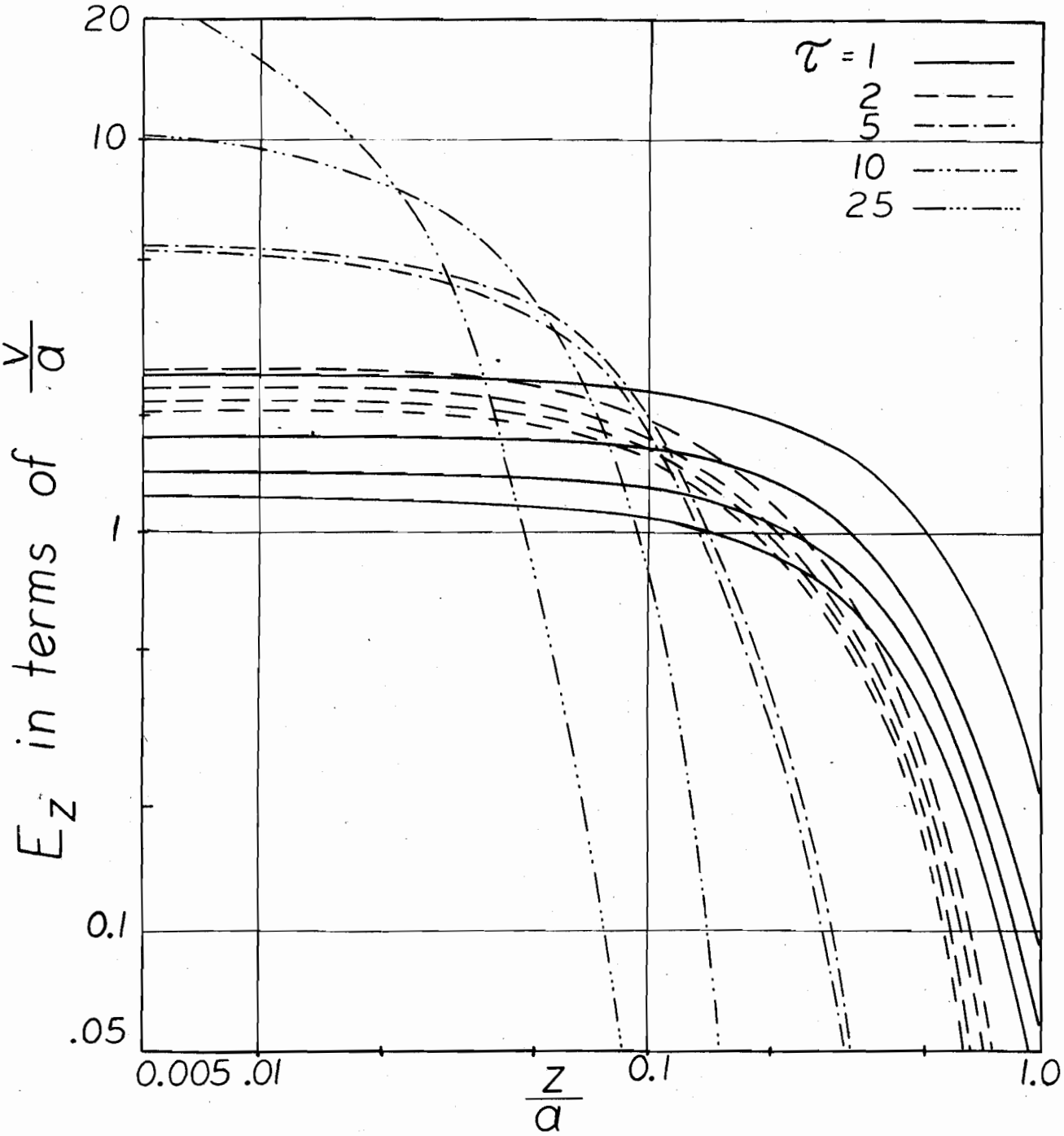
20
10
1
0.1
.05
0.005
.01
0.1
1.0
E_z in terms of $\frac{V}{a}$
$\frac{z}{a}$
$\tau = 1$
2
5
10
25

Fig. 3

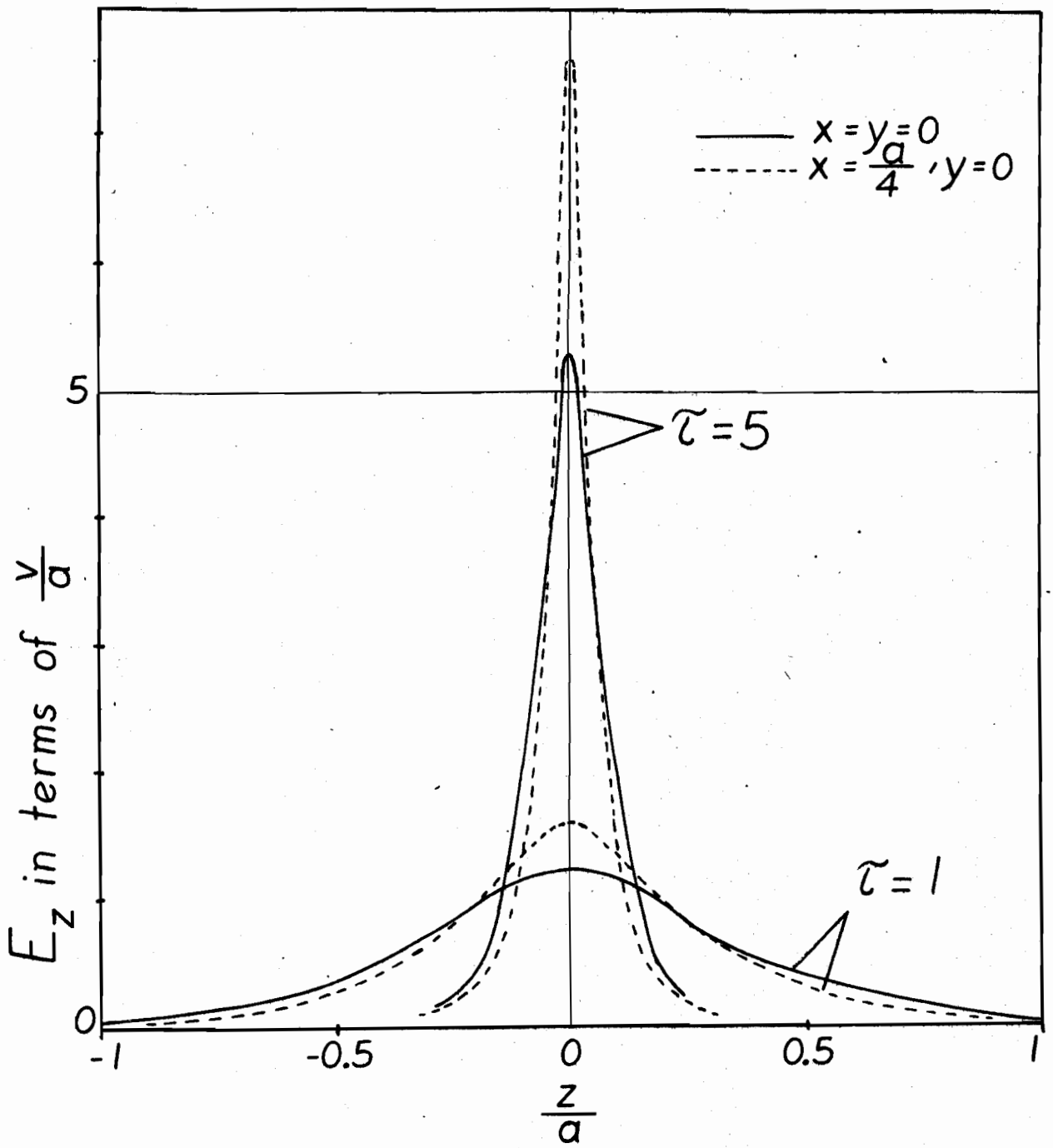

FIG. 4.

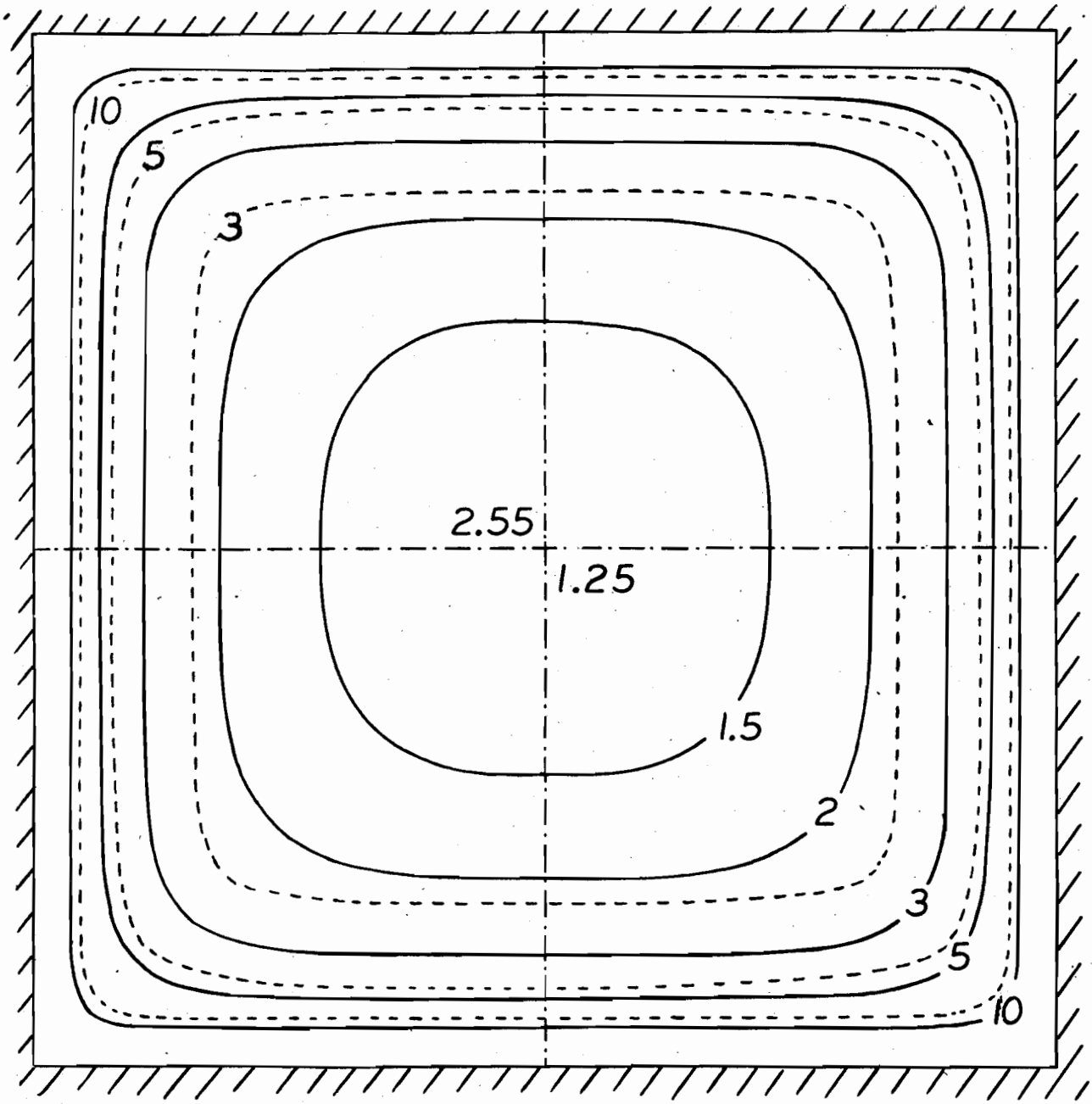

$\tau = 1$

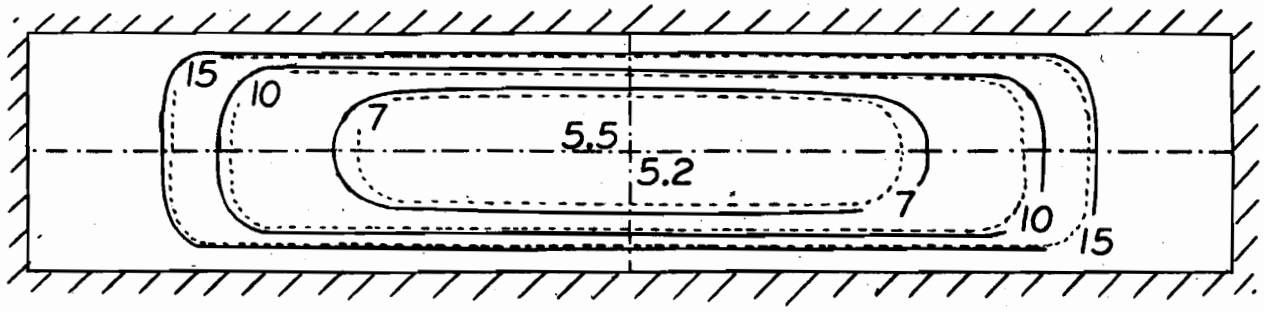

$\tau = 5$

Fig. 5

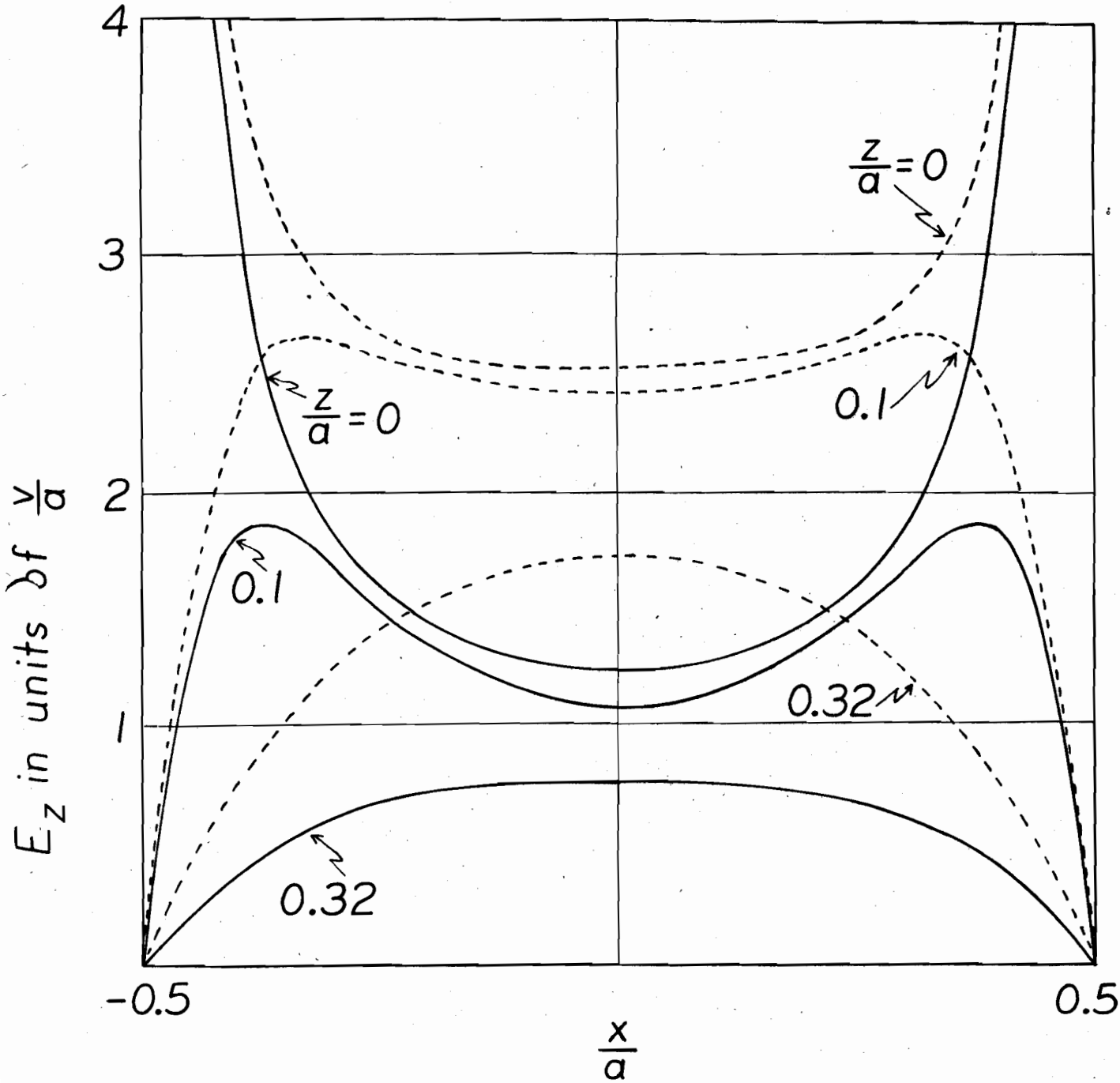
4
3
2
1
-0.5
0.5
E_z in units of $\frac{V}{a}$
$\frac{x}{a}$
$\frac{z}{a}=0$
$\frac{z}{a}=0$
0.1
0.1
0.32
0.32

Fig. 6

Fig. 7

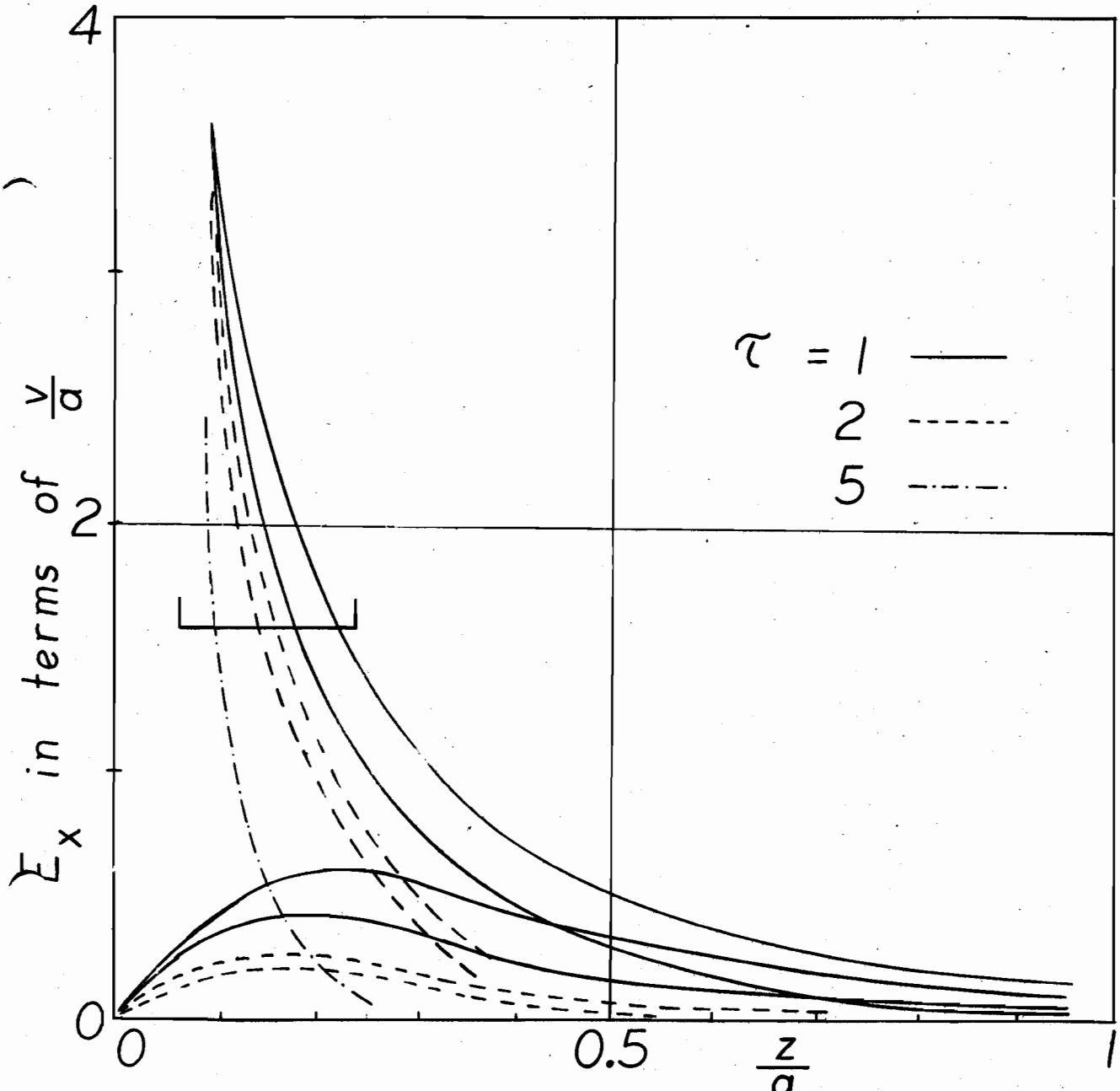

Fig. 8

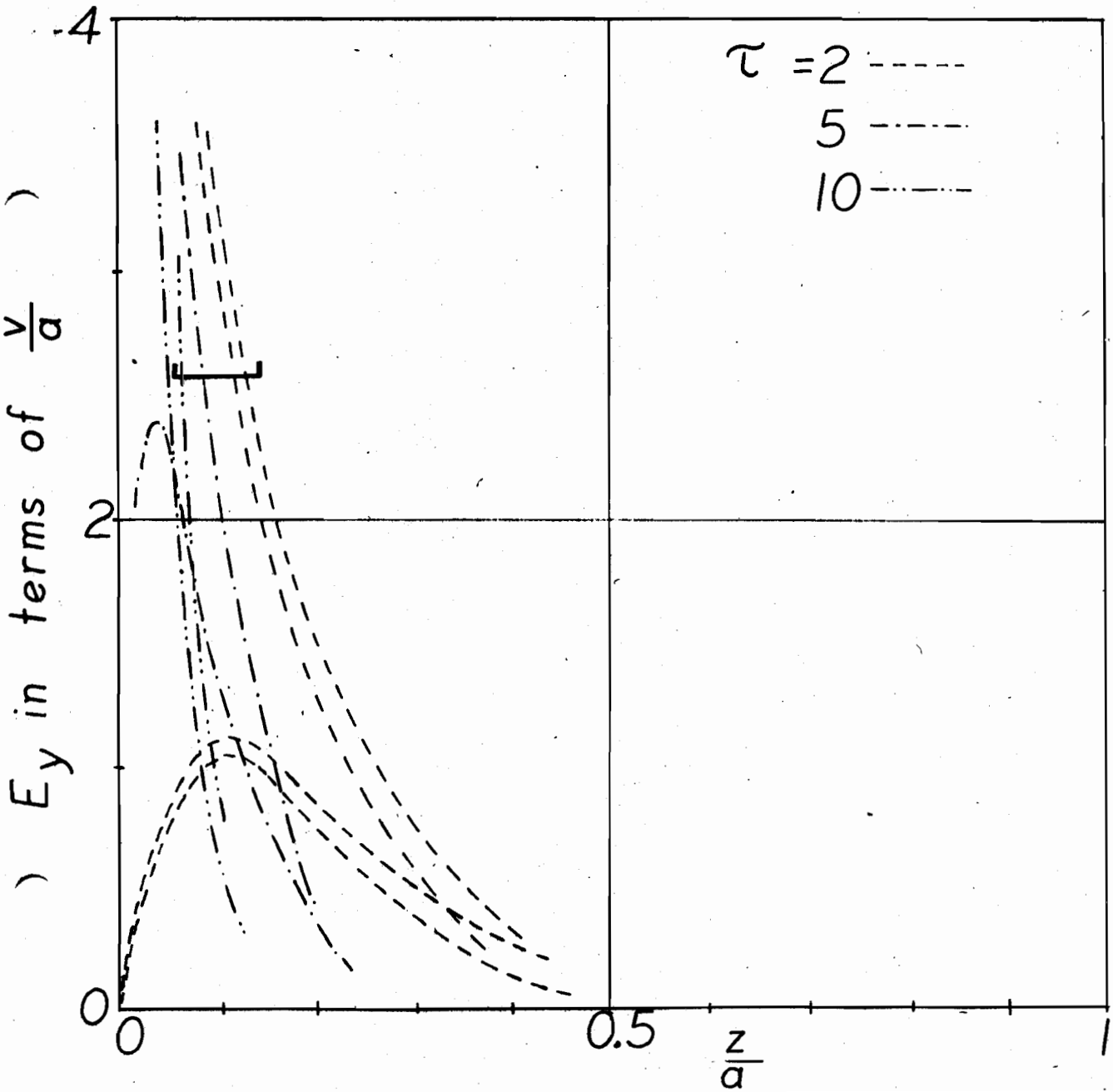

Fig. 9

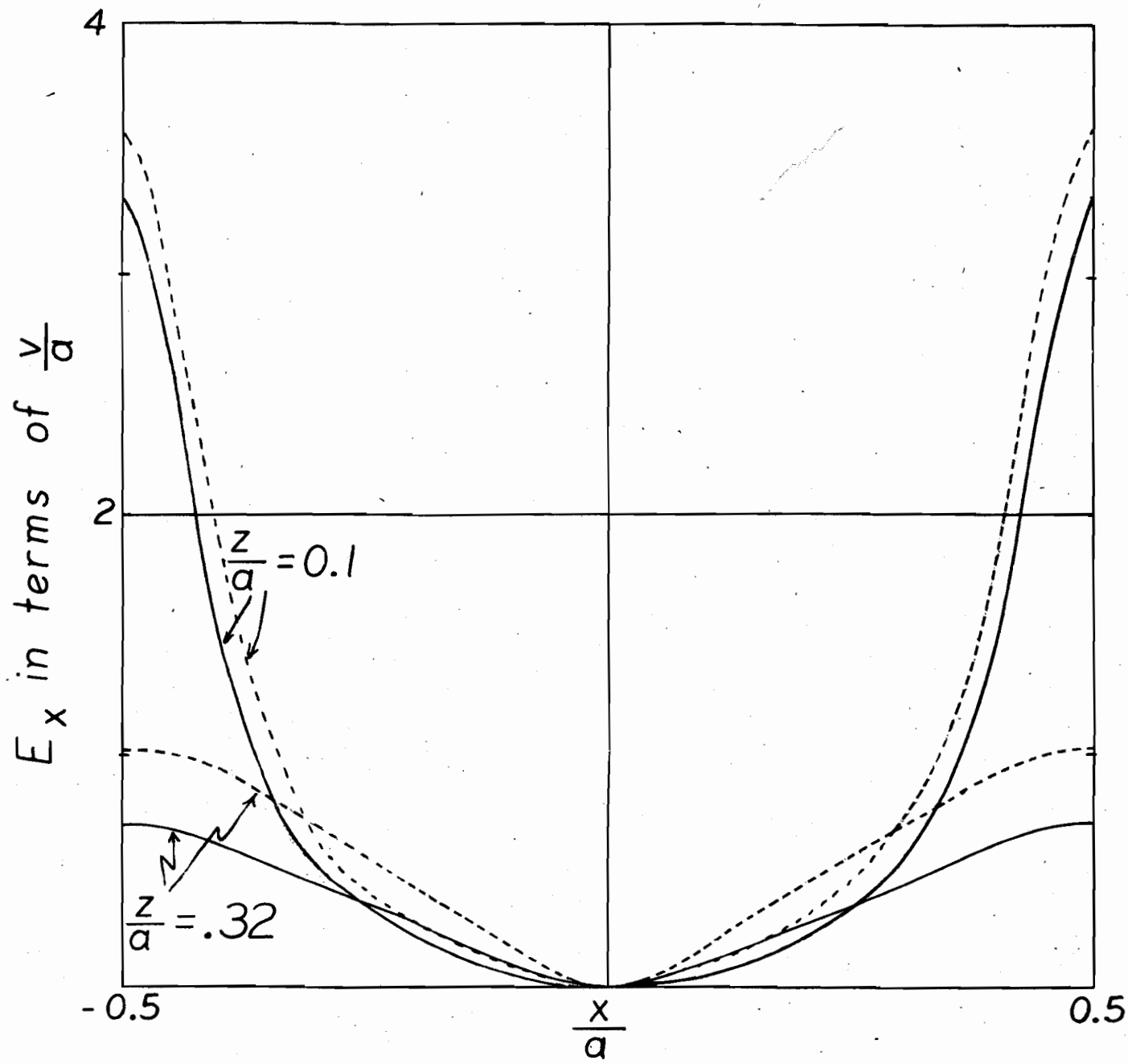

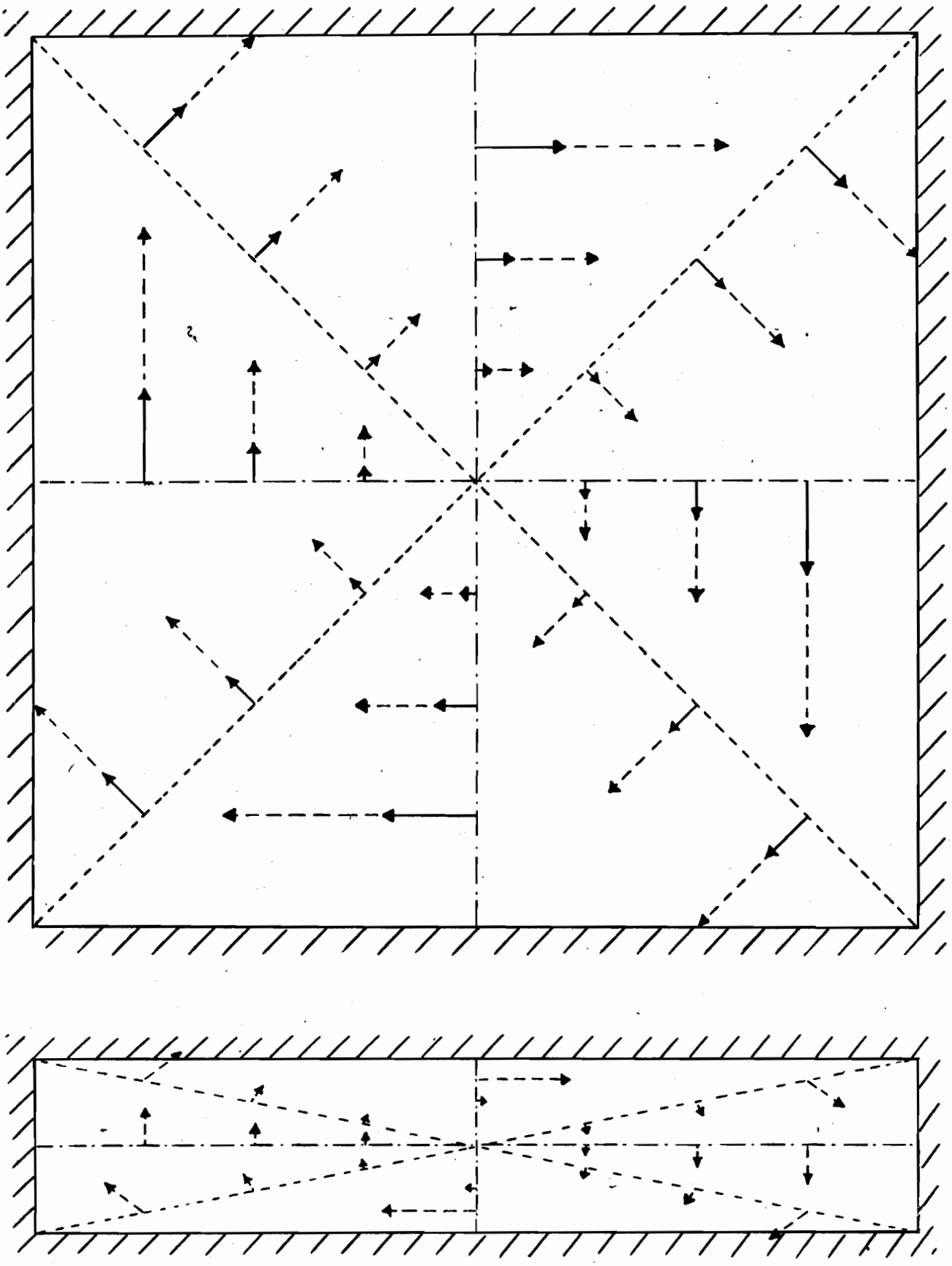

Unit of magnetic field: $H = Y_0 \cdot \frac{V}{a}$

Fig. 10

Fig. 11

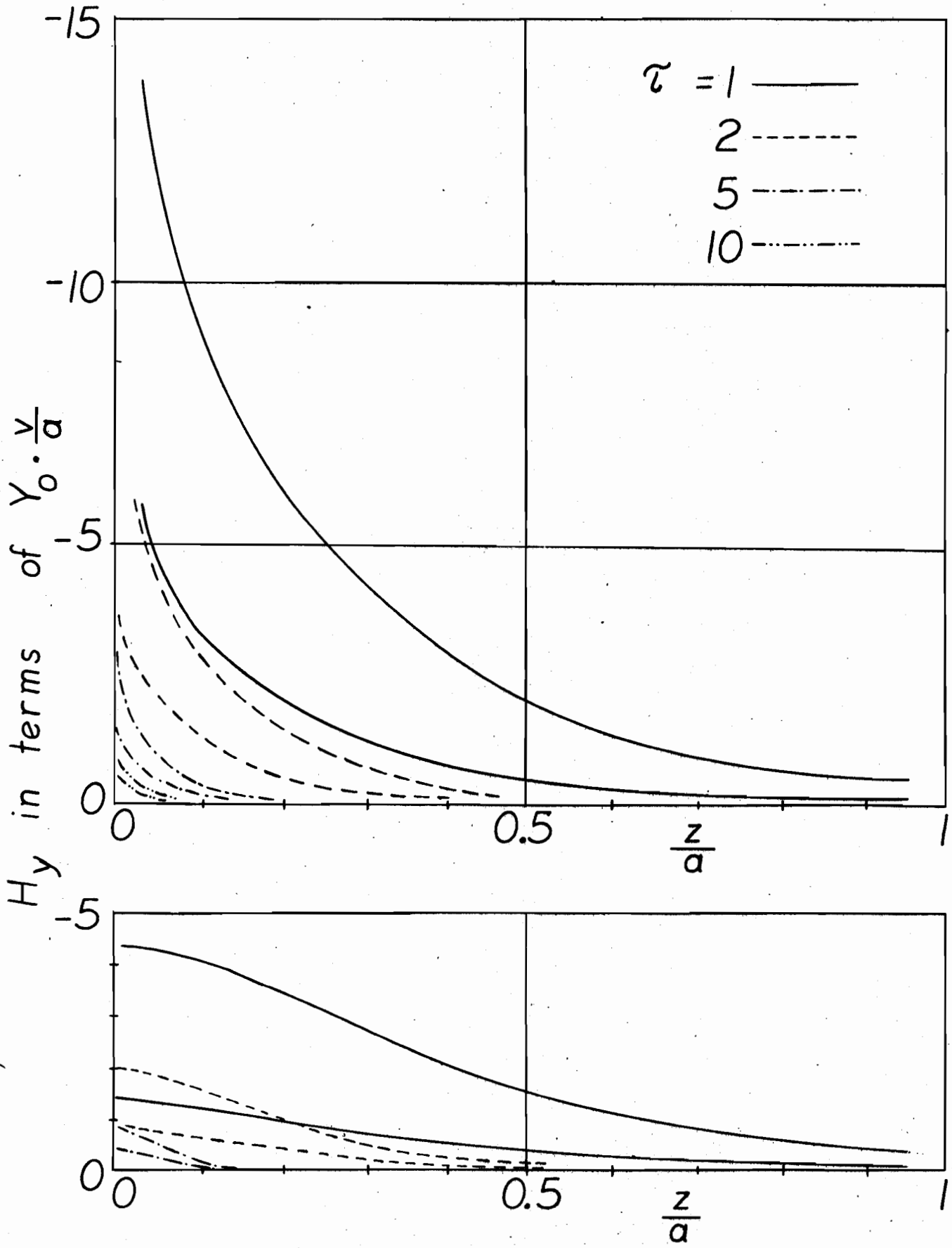
-15
-10
-5
0
τ = 1
2
5
10
H_y in terms of $Y_0 \cdot \frac{v}{a}$
0
0.5
1
$\frac{z}{a}$
-5
0
0
0.5
1
$\frac{z}{a}$

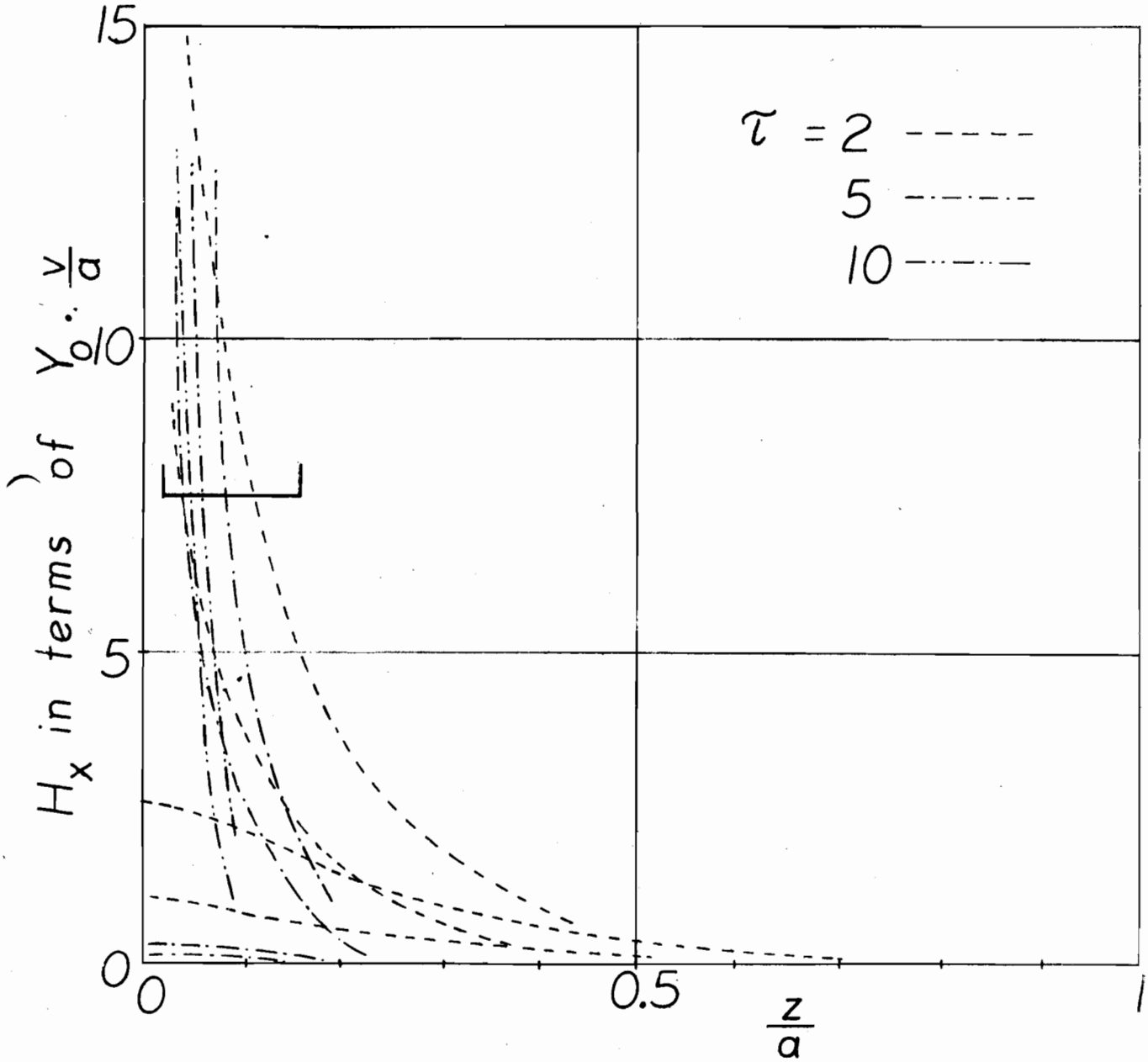

Fig. 12

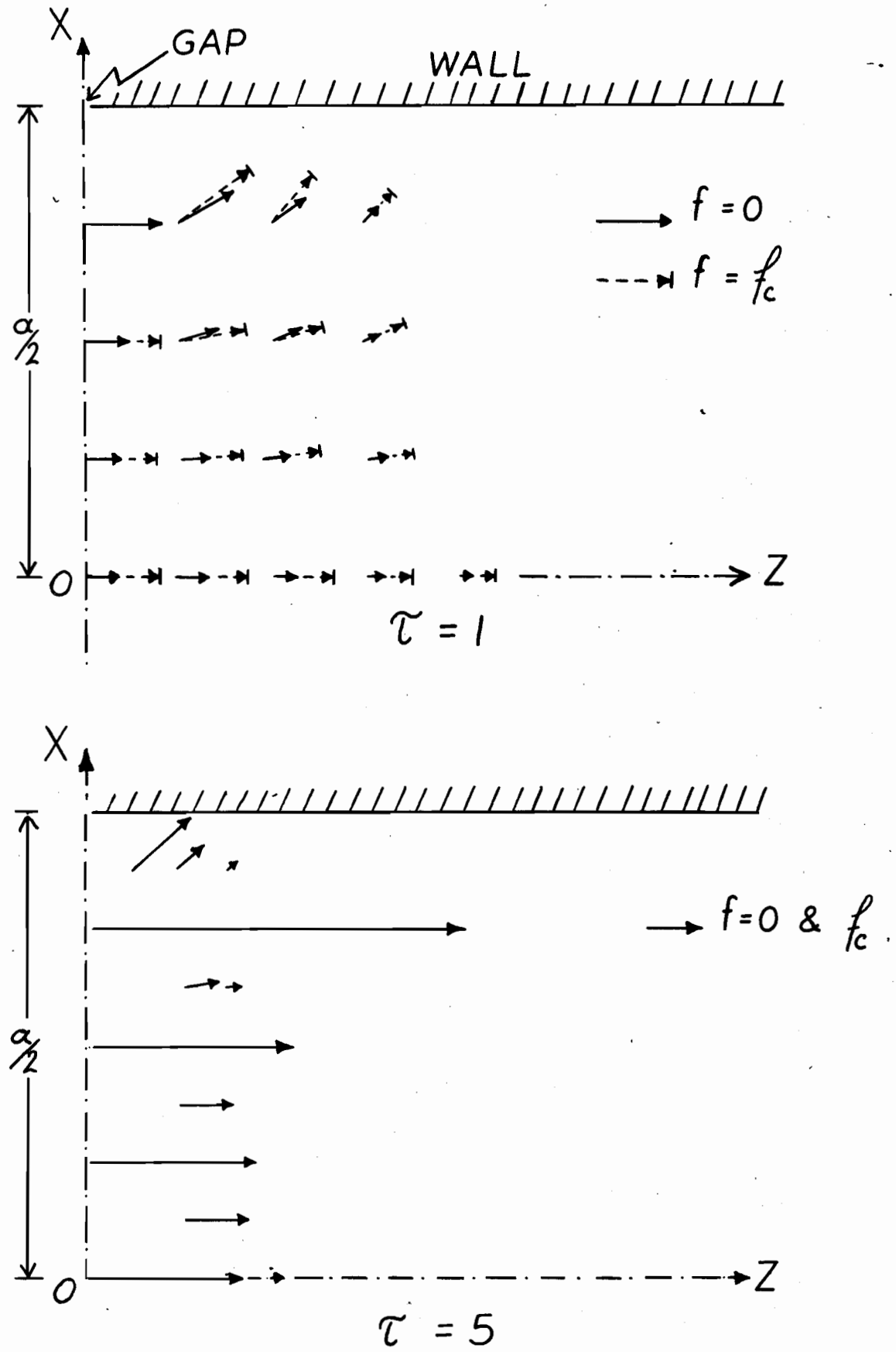

Scale of electric field ⊢ V/a

⊢——⊣ 5 V/a

Fig. 13

FIG. 14

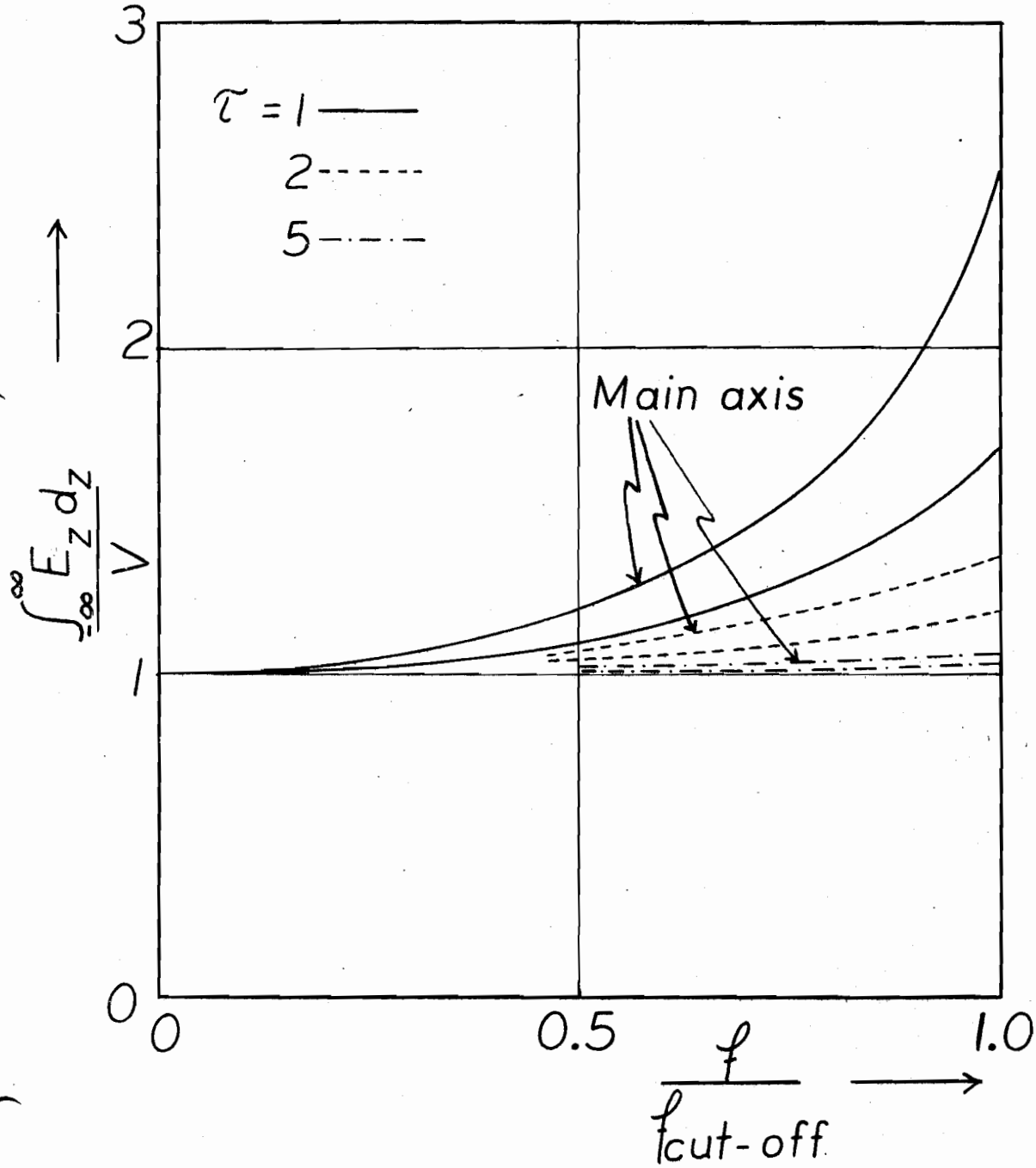
3
2
1
0
$\tau = 1$
2
5
Main axis
$\int_{-\infty}^{\infty} E_z \, dz / V$
0
0.5
1.0
$f / f_{cut\text{-}off}$